Advances in Computational Design, *Vol. 10, No. 4 (2025) 375-388*
https://doi.org/10.12989/acd.2025.10.4.375

Advancing neuroblastoma diagnosis in paediatrics: Utilizing CNN-GRU and machine learning for improved detection and prediction

Dhiyanesh B.*[1], Janani I.[2], Prakash S.P.[3], Divya K.[4] and Gomathi S.[5]

[1]*Department of CSE Emerging Technologies, SRM Institute of Science and Technology, Vadapalani Campus, Chennai, Tamil Nadu India*
[2]*Sona College of Technology, Salem, Tamil Nadu, India*
[3]*Bannari Amman Institute of Technology, Erode, Tamil Nadu, India*
[4]*Karpagam Institute of Technology, Coimbatore, Tamil Nadu, India*
[5]*Dr. N.G.P. Institute of Technology, Coimbatore, Tamil Nadu, India*

(Received July 29, 2025, Revised September 23, 2025, Accepted October 19, 2025)

Abstract. Neuroblastoma is the most common extracranial solid malignancy in children. It is possible to estimate the cancer's unpredictable biological activity based on the patient's age, genetic makeup, the biology of the cancer, and the extent of disease at diagnosis. Machine learning algorithms have the potential to enhance the precision and efficacy of cancer diagnosis, individualized therapy selection, and long-term outcome prediction. A subset of machine learning known as Artificial Intelligence (AI) is capable of spotting patterns in data and acting without the need for special programming to accomplish predetermined objectives. The patient populations most likely to benefit from advanced imaging tests may be enriched, high-risk populations can be identified, and individualized screening tests can be prescribed with the aid of machine learning technologies. Modern computational tools are becoming more and more crucial in pediatric oncology because of their invasive nature and the requirement for an early and precise diagnosis. Convolutional Neural Networks (CNNs) and Gated Recurrent Units (GRUs) are two methods that can be used to increase the precision and predictability of detection. The Grey-Level Cooccurrence Matrix (GLCM) extracts the features as energy, entropy, dissimilarity, homogeneity, and contrast. The CNN-GRU to produce the results as precision, recall, accuracy, and F1-score 93%, 80%, 95%, and 83%.

Keywords: cooccurrence matrix; imaging analysis; neural network; neuroblastoma; pediatric oncology; texture feature

1. Introduction

The second most prevalent cancer in newborns and early childhood is Neuroblastoma (NB). It appears as a sympathetic nervous system tumor. About 60% of these tumors exist in the abdomen, while 50% are found in the adrenal gland medulla.

Locoregional tumors (L1 and L2) exhibit the presence or absence of Image-Defined Risk Factors (IDRFs), which are the foundation for non-B staging in accordance with the International Neuroblastoma Risk Group Staging System (INRGSS). Visible on radiographic images are known

*Corresponding author, Associate Professor, E-mail: dhiyanu87@gmail.com

 ISSN: 2383-8477 (Print), 2466-0523 (Online)

as identifiable surgical risk factors, or IDRFs. When it comes to infants under 1.5 years old, M exhibits extensive disease, whereas MS affects L1 and L2, with metastases restricted to the skin, liver, and bone marrow (but not cortical bone) (Leila Jahangiri *et al*. 2024).

The use of Artificial Intelligence (AI) is expanding quickly across several industries, including pediatric oncology, as a result of cheaper and more powerful computers. Central nervous system cancers and diagnostic imaging are the AI applications that are being researched the most. Process mining, clinical route modeling, and computer-interpreted guidelines, however, need strong supporting data. Though there are still obstacles to overcome, such as the requirement for sizable datasets for algorithm training, the application of AI in pediatric cancer is expanding quickly (Tozzi *et al*. 2022).

To use of Magnetic Resonance Imaging (MRI) to identify primary brain tumors in pediatric patients is investigated by Artificial Intelligence (AI). Algorithms for machine learning were used to test the remaining 30%. According to radiologist reports, the Artificial Neural Network approach proved to be accurate in identifying children's primary brain tumors (Hamd *et al*. 2024) Using tiny tabular datasets, the study created an interpretable machine learning framework to predict infection in pediatric AML and ALL (Al-Hussaini *et al*. 2024).

The findings demonstrated that VOI-based measurements could reliably distinguish between tumor subtypes and had reduced variability across all DKI indicators than ROI-based measurements (Voicu *et al*. 2024, Prashantha *et al*. 2021). A quantitative method for analyzing medical imaging data is offered by radiomics, which expands on the information obtained from pixel/voxel grey-level values and their interactions. The “radiomic workflow” entails the collection of images, the extraction and selection of features, and the training of prediction models CNN to test the features that have been chosen (Pacchiano *et al*. 2024).

2. Related work

(Yearley *et al*. 2022) Machine learning methods may expedite and enhance the diagnosis process for Posterior Fossa Tumors (PFTs). The algorithms demonstrated inconsistent performance according to the specific tumor types, classifier(s) employed, and sample size. The most examined cancers were pilocytic astrocytoma, medulloblastoma, and ependymoma; algorithm accuracies ranged from 37.5% to 94.5%. Small sample numbers, unequal tumor type representation, unreliable performance reporting, and lack of practical application are some of the shortcomings, though.

(Ramesh *et al*. 2021) 42 different publications were found in the databases of Embase, Scopus, and Medline; 20 of these looked at CNS tumors, 13 at solid tumors, and 9 at leukemia. Among the machine learning tasks were classification, treatment response prediction, and dose optimization.

(Chadaga *et al*. 2023) Using ML and Descriptive Artificial Intelligence (XAI) to Predict Survival Probability in Children Undergoing Hematopoietic Stem Cell Transplantation. This model gave optimal results in terms of precision, accuracy, recall, and AUC. XAI identified significant features including recurrence, recipient and donor age, and platelet recovery time.

(Steyaert *et al*. 2023) The analysis of biological data has improved with the use of deep learning in imaging and genomics, especially for complicated disorders like cancer. A DL framework predicts the prognosis of brain tumors by integrating genetic and imaging data. In comparison to single data models, the framework produced improved prediction results by fusing gene expression profiles with histopathological pictures. Additionally, more pertinent biological

pathways were found by the model.

(Yang *et al*. 2021) Tumor purity in juvenile CNS tumors is a topic that needs more research. Researchers used the Infinium Purify algorithm, random forest machine learning, and the evaluation technique to assess tumor purity in pediatric datasets. The results showed how CNS tumor purity is typically distributed and how it relates to both molecular and clinical indicators. Three immune-related genes had a negative correlation with MB purity, whereas immunotherapy-associated indicators did not demonstrate any clear relationship with MB purity.

(Artzi *et al*. 2021) Differentiating between the many forms of Posterior Fossa Tumors (PFT) that are typical in youngsters is crucial. For PFT classification, a study suggested a coupled architecture made up of a table-based network and a pre-trained ResNet-50 CNN. Data was collected from 136 pediatric patients with 158 MRI scans and a PFT diagnosis. The best classification results were obtained using the CNN + table data structure, with an average cross-validation accuracy of test and validation dataset as 0.87 ± 0.02 and 0.88 ± 0.04

(Zhang *et al*. 2020) The advancement of technology in medicine, particularly biotechnology and artificial intelligence, has substantially benefited lives. Scholars are investigating the application of deep learning algorithms, particularly CNN, to identify and diagnose pediatric cancer, an arduous disease to identify just from symptoms. The usefulness of these algorithms in identifying and treating pediatric tumors is investigated in this work.

(Zheng *et al*. 2024) The overall survival rates of pediatric lymphoma patients have significantly increased, according to a study that examined data on the disease from 1975 to 2018. Important risk variables were found, and a nomogram with predictive values was created. In terms of predicting survival, the nomogram performed better than the Ann Arbor stage method. Additionally, machine learning models fared better in forecasting the risk of death specific to lymphoma than traditional methods did. After ten years, survivors of pediatric cancer had a lower chance of developing lymphoma but a higher chance of developing non-lymphoma illnesses.

(Talaat and Gamel 2021) The article offers an attention-augmented algorithm for blood cancer diagnosis in children (A2M-LEUK), which enhances leukemia cell detection and classification by utilizing machine learning and image processing approaches based on attention mechanisms. The algorithm's performance metrics, which included accuracy of 99.98%, F1-score of 99.98%, recall of 100.00%, and precision of 99.97%, were outstanding. This novel strategy may lighten the strain on medical personnel while enhancing the identification and management of pediatric leukemia.

(Zhang *et al*. 2023) This work presents the Random Survival Forest (RSF) ML model for analysing survival in young adult, adolescent, and pediatric cancer survivors. Regarding pediatric survival and second malignancy, the model's average Concordance index is 92.9% and 86.8%, respectively. This implies that by swiftly identifying high-risk individuals, machine learning models can reduce the workload of physicians.

(Jiwani *et al*. 2023) An enhanced computational deep learning model for pattern detection in acute Lymphoblastic Leukemia (LL) has been presented to find patterns in white blood cell count data. The model demonstrated 81.53% and 87.92% efficiency in the delivery of chemotherapy, 79.16% and 94.31% efficiency in the management of stem cell transplants, 63.77% and 87.37% efficiency in the delivery of radiation treatment, and 88.92% and 85.92% efficiency in the administration of drugs.

(Zijtregtop *et al*. 2023) A 12-factor diagnostic score system was created utilizing information from 181 kids who were referred to a pediatric oncology center to identify high-grade lymphoma in kids with cervical lymphadenopathy. The model, which combined 29 potential cancer-predictive variables, demonstrated an 88% specificity and 95% sensitivity in identifying both Non-Hodgkin

Lymphoma (NHL) and Classical Hodgkin Lymphoma (CHL). This strategy may facilitate prompt referrals and minimize needless invasive operations for patients with benign lymphadenopathy.

(Yoon *et al*. 2022) Using the ICD-O-3 coding system, researchers created deep learning-based algorithms for information extraction from cancer pathology reports. Using data from 29,206 reports from six state cancer registries, they assessed these models. With a micro-F1 score of 0.987, the results demonstrated that direct ICCC (International Classification of Childhood Cancer) classification performed much better than utilizing the ICD-O-3 model again.

(Chounta *et al*. 2023) Explored the use of dosiomics signatures to understand the spatial characteristics of cardiac doses associated with Valvular Heart Disease (VHD) in childhood cancer survivors. Scientists analyzed data from the French Childhood Cancer Survivors' Study and found that dosiomics-based models and Mean Heart Dose (MHD) performed similarly globally. When dosiomics features were applied, the prediction power for subpopulations with spatially diverse dose distributions was greatly increased. The results may be applied to customized follow-up recommendations and VHD risk assessment using machine learning methods.

(Jian *et al*. 2023) A powerful chemotherapy medication called High-Dose Methotrexate (HD-MTX) is used to treat children with Acute Lymphoblastic Leukemia (ALL). However, it could result in harmful drug-related issues and a postponement of elimination. The purpose of this research was to identify the risk factors linked to delayed MTX elimination and to create a predictive tool. In a 329-person experiment, 1400 individuals had delayed MTX elimination. The SMOTE-based XGBoost technique has an AUROC of 0.788 in the external validation, which is higher than the other models.

(Yang *et al*. 2024) As far as predicting T-cell lymphoma goes, the PET/CT-based model fared better than the SUV/CT-based model. The PET/CT-based model showed very good accuracy, AUC, and good fit across patient and lesion levels. This suggests that 18FFDG PET/CT-based radiomics models are valuable over SUV-related characterization.

(Bohannan *et al*. 2022) Random Survival Forest (RSF) has been presented to expect relapse/death in high-risk pediatric B-ALL patients. It makes use of 156 patients' full exome sequencing profiles, which provide interpretable genomic inputs. Seven genomic areas were shown to be the most predictive of either a relapse or a death-free survival; a polygenic score derived from the top seven variables successfully divided the patients into two groups. 174 standard-risk patients were used to verify the model.

(Horan *et al*. 2023) Ten considerations for evaluating Patient-Reported Outcome Measures (PROMs) in the treatment of pediatric cancer survivors are offered to doctors in this article. It highlights the need to select the appropriate therapeutic response measure and strategy while taking into account realistic obstacles and solutions. The use of cutting-edge technologies to incorporate PROMs into clinical workflows is also highlighted in the article.

(Kifle *et al*. 2023) Surgery to remove the brain tumor is the most common course of treatment; however, biopsy tissue samples can be time-consuming and unreliable. Snapshot Hyperspectral Imaging (sHSI) cameras can provide real-time guidance to patients in their teens on how to distinguish between healthy brain tissue and abnormalities. The specificity of tumor segmentation was 0.996, while the visible and infrared HSI models came in at 0.91 and 0.93, respectively. The average Intersection of Unions (IoUs) for the RGB, infrared sHSI, and visible sHSI models were 0.76, 0.59, and 0.57, correspondingly.

(Li *et al*. 2024) The study looks into the function of migrasomes in neuroblastoma, a common childhood malignant tumor. It finds genes and creates the MigScore machine-learning model, which forecasts immunological reactions and medication compatibility. The findings indicate a

strong negative correlation between MigScore and clinical results, indicating the importance of microsomes in the prognosis of neuroblastoma.

(Attallah 2021). Three TL CNN are used by the system to generate spatial TL features. Time-frequency characteristics are then extracted from these features using Discrete Wavelet Transform (DWT), and the features are then combined using Discrete Cosine Transform (DCT) and Principal Component Analysis (PCA).

(Cheng *et al*. 2024) The goal of the project was to use blood samples, critical leukemia indications, and nutritional biomarkers to create an early predictor for childhood leukemia. It discovered significant variations in markers between youngsters in good health and those with leukemia using a machine-learning technique. The AUC for leukemia subtypes and AML prediction was 0.950 and 0.909, correspondingly, signifying the potential of AI in contemporary medicine.

(Vekariya *et al*. 2022) It is anticipated that liver cells from Liver Hepatocellular Carcinoma (LIHC), the third most common cause of cancer-related mortality, will express genes in a certain way using machine learning techniques. Open-source methods were used to acquire data from RNA sequences, the human genome, histones, and methylation. With an AUC of 1.0 and a 99.67% accuracy rate in predicting liver cancer using XGBoost classification.

3. Proposed methodology

To increase prediction accuracy, a combination of sophisticated image processing and machine learning approaches is used for the analysis of neuroblastoma in pediatric tumors. Medical images are first preprocessed using a Wiener filter to lower noise and enhance image clarity. The Gray Level Co-occurrence Matrix (GLCM) is then used to extract texture characteristics from the denoised images, capturing crucial information about the texture of the malignancy. After that, a convolutional neural network (CNN) is fed these characteristics to extract spatial features. Utilizing a Synchronized Recurrent Unit the sequential or temporal components of the picture data are handled. By combining both methods, the CNN-GRU model successfully classifies images of neuroblastomas and yields vital details about the features of the malignancy. Figure 1 depicts the architecture of the suggested methodology.

3.1 Dataset

With a median age of diagnosis of 17 months, neuroblastoma is the most common tumor of the sympathetic nervous system and the most frequent juvenile malignancy. It accounts for fifteen percent of pediatric cancer mortality. The International Neuroblastoma Staging System (INSS), which is based on surgical resection, is used in the United States to stage neuroblastomas.

3.2 Preprocessing: Wiener filter

Wiener filter is a powerful tool used in image pre-processing for noise reduction and image enhancement. This is particularly useful in situations where the image is distorted by additive noise and/or blurring. A Wiener filter is designed to reduce noise in an image while preserving important details. It works by estimating the original image from a noisy version using a statistical approach. To minimize the error between original image and estimated image.

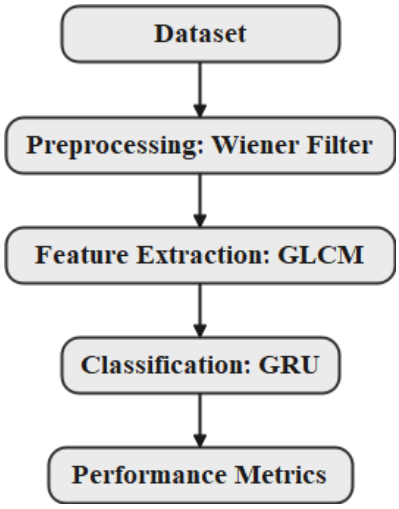

Fig. 1 Flow diagram of the proposed methodology

The Wiener filter is based on the concept of filtering in the frequency domain. Before using the Wiener filter, the power spectra of the original image and the extra noise need to be determined. The power spectrum of white additive noise and noise variance are identical. The power spectrum of the source image can be estimated using a variety of techniques. The filter is defined as:

$$H(u,v) = \frac{S_f(u,v)}{S_f(u,v) + S_n(u,v)}$$
$$H(u,v) - wiener\ filter\ in\ the\ frequency\ domain,$$
$$S_f(u,v) - power\ spectral\ density\ of\ an\ original\ image,$$
$$S_n(u,v) - power\ spectral\ density\ of\ noise. \quad (1)$$

3.3 Feature extraction: GLCM (Gray-Level Cooccurrence Matrix)

A statistical technique called the GLCM is used to examine the spatial correlations between pixels in an image to assess its texture. It is especially useful for recognizing anomalies, such as cancers, and defining tissues in medical imaging. For neuroblastoma image feature extraction, several mathematical Eqs. are used to calculate texture features using GLCM. Here is a detailed explanation of how these features are calculated:

Contrast:

Contrast measures local variations in the GLCM. It is defined as: below Eq. 2.

$$contrast = \sum_{i,j} (i-j)^2 . P'(g_i, g_j) \quad (2)$$

Energy

Energy, sometimes referred to as the angular second moment, evaluates the uniformity that the GLCM, as below Eq. 3.

$$Energy = \sum_{i,j} [P'(g_i, g_j)]^2 \quad (3)$$

Homogeneity

The degree to which the distribution of the GLCM's elements is close to the diagonal is measured by homogeneity, as below Eq. 4.

$$Homogeneity = \sum_{i,j} \frac{P'(g_i, g_j)}{1 + (i-j)^2} \tag{4}$$

Entropy

Entropy is calculated as the probability distribution of pairs of gray-levels, $P'(g_i, g_j) log_2(P'(g_i, g_j))$, of which pairs with zero probability are ignored to remove errors. A higher entropy represents more irregular and complex textures, whereas a lower value represents uniformity, as below Eq. 5.

$$Entropy = -\sum_{i,j} P'(g_i, g_j) log_2(P'(g_i, g_j)) \tag{5}$$

Dissimilarity

Dissimilarity measures the difference between gray levels, as below Eq. 6.

$$Dissimilarity = \sum_{i,j} |i-j| . P'(g_i, g_j) \tag{6}$$

3.4 Classification:

A. CNN (Convolution Neural Network)

Designing a Convolutional Neural Network (CNN) for medical image analysis involves developing a specialized framework to handle the unique challenges of medical imaging, such as high-dimensionality and subtle features in images. Typically, CNN for medical images starts with an input layer that accepts preprocessed grayscale or color images. The network uses a series of ordered layers to automatically learn and extract hierarchical features from images, such as edges and textures, using small filters (eg, 3×3 or 5×5). These convolutional layers are followed by activation functions such as ReLU.

Convolutional layer: The initial layer of CNN is in charge of identifying little details in the image, such as corners and edges. It creates feature maps that highlight distinct aspects of the input image by applying a variety of filters to it.

Pooling layer: After the convolutional layer, the pooling layer keeps the most important features while reducing the dimensionality of the feature maps. It reduces the size of feature maps by performing under-sampling techniques like maximum pooling, which helps to lower the computational load and manage overfitting.

Fully Connected Layer: This layer incorporates all the features that have been learned from the previous layers after dimensionality reduction and feature extraction. To integrate the recovered features into a complete representation that can be used for classifiers or regression, each neuron in this layer is connected to all other neurons in the previous layer.

To alleviate overfitting during training, a dropout layer is frequently introduced. By randomly deactivating a portion of the neurons, this layer helps the network become less dependent on any one neuron and improves its ability to adapt to new information. Furthermore, activation functions are crucial for enhancing network efficiency. Due to its ability to produce nonlinearity by delivering positive values unmodified and producing zero for negative inputs, the Rectified Linear

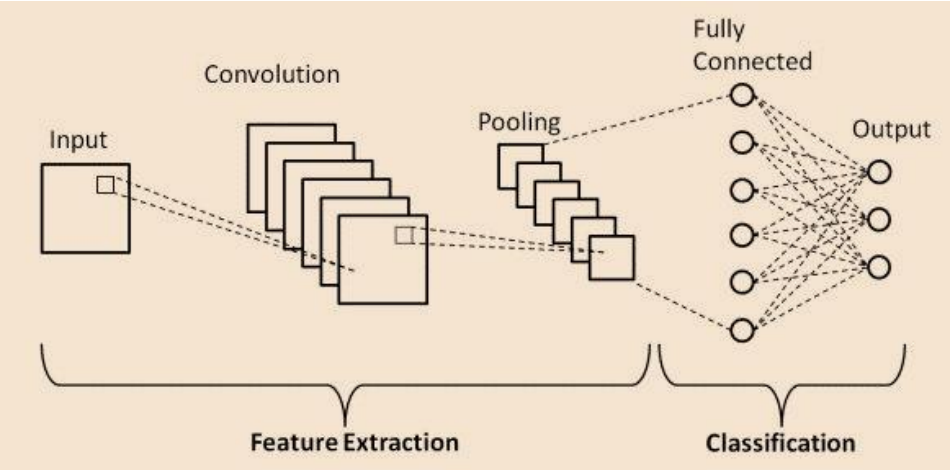

Fig. 2 Architecture of CNN

Unit (ReLU) is a widely used option. And lastly, the output layer frequently uses the Softmax activation function for multi-class classification issues. This function transforms the network output into a probability distribution across several classes. CNNs can be effectively trained to achieve excellent performance in applications like object detection and picture classification by combining this layered method with techniques like dropout and appropriate activation functions.

B. GRU (Gated Recurrent Unit)

GRU is a subset of Recurrent Neural Networks (RNN), which is primarily designed to handle long-term memory and gradients in backpropagation problems. Because GRU only has two gates an update gate and a reset gate it is easier to understand, requires less processing power, and trains more quickly. The reset gate controls how long the prior data is kept around. The reset gate will increase in value the more historical data that is ignored. To control how the recent new cell state is influenced by the previous cell state and the recent new input, use the update gate which is shown in Figure 3.

The computation of the update gate, which uses the sigmoid function to determine how much of the previous hidden state needs to be updated, is the first stage in the GRU process. It consists of the current input and the hidden state of the previous state. The update gate can be expressed mathematically, as below Eq. 7.

$$z_t = \sigma(W_z.[h_{t-1}, x_t] + b_z) \tag{7}$$

Whereas,
$z_t - update\ gate$,
$\sigma - Sigmoid\ function$,
$W_z - Weight\ matrix$,
$x_t - current\ input$,
$h_{t-1} - previous\ hidden\ state$,
$b_z - bias\ for\ update\ gate$,
$[h_{t-1}, x_t] - Concatenation.$
The reset gate calculation is expressed below the Eq. in the update gate, as below Eq. 8.

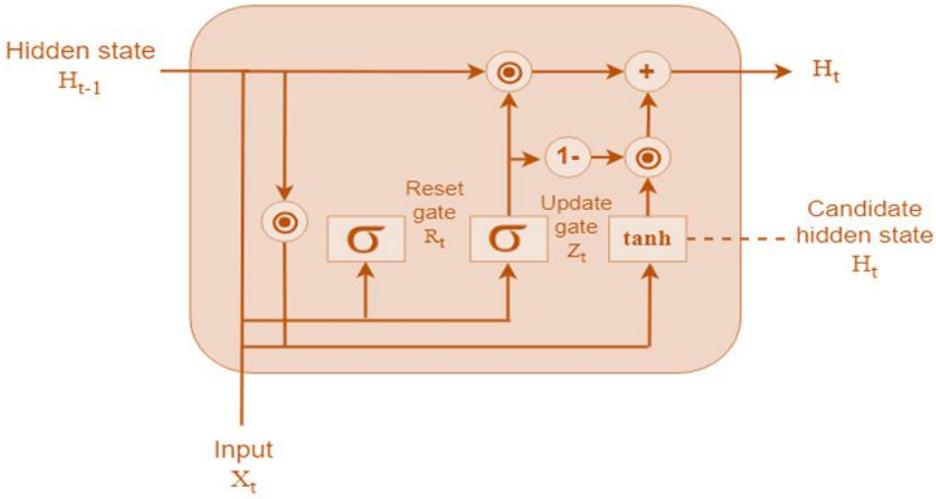

Fig. 3 GRU Architecture

$$r_t = \sigma(W_r.[h_{t-1}, x_t] + b_r) \tag{8}$$

In this context, features like age, blood pressure, blood urea, serum creatinine, and others specific to CKD diagnosis are considered. This tailored application ensures the KNN algorithm accurately reflects the patterns and proximities relevant to chronic kidney disease detection.

Here,

$r_t - Reset\ gate\ vector$,

$W_r - Weight\ matrix\ for\ reset\ gate$,

$b_r - Bias\ for\ the\ reset\ gate$.

Following the computation of the reset gate, a candidate hidden state is generated using the hyperbolic tangent function (tanh). The effect of the previous concealed state is determined by the reset gate value, as below Eq. 9.

$$h'_t = \tanh\,(W.[r_t * h_{t-1}, x_t] + b) \tag{9}$$

Here,

$h'_t - Candidate\ hidden\ state$

$b - bias$

$W - computation\ on\ the\ weight\ matrix$

After the reset gate is calculated, a candidate hidden state is generated using the hyperbolic tangent (tanh) function. The effect of the previous hidden state is determined by the value of the reset gate, as below Eq. 10.

$$h_t = (1 - Z_t) * h_{t-1} + Z_t * h'_t \tag{10}$$

The expression of GRU used the sigmoid function in the update and reset gates to determine what diagnostic features of paediatric neuroblastoma should be retained or forgotten. The tanh candidate generation function tanh is a non-linear medical pattern capturing function that creates candidate hidden states. These two functions are in a synergizing process to balance between the past and new information. This allows the GRU to model intricate biomarker and imaging

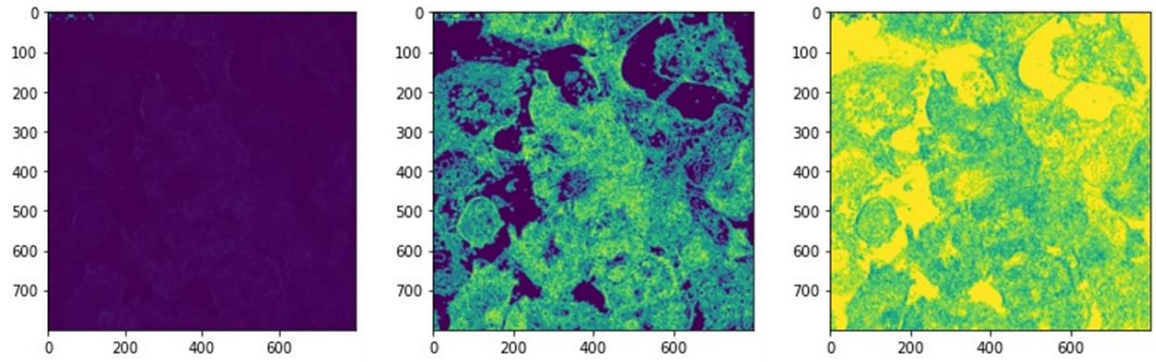

Fig. 4 Contrast, entropy, homogeneity

indications to allow precise diagnosis, as below Eqs. 11 and 12.

$$\sigma(x) = \frac{1}{1 + e^{-x}} \tag{11}$$

$$\tanh(x) = \frac{e^{2x} - 1}{e^{2x} + 1} \tag{12}$$

4. Result and discussion

The proposed Pediatric neuroblastoma cancer classification is based on a hybrid CNN- GRU algorithm implemented in Python language. The preprocessing is a wiener filter, feature extraction as GLCM, and classification as hybrid CNN-GRU.

Performance metrics

Accuracy

The percentage of cases that were correctly classified out of all the instances.

$$Accuracy = \frac{TruePositive + True\ Negative}{True\ Positive + True\ Negative + False\ Positive + False\ Negative}$$

Precision

The ratio of true positive cases to all cases classified as positive

$$precision = \frac{TruePositive}{TruePositive + False\ Positive}$$

Recall

True positive instances as a percentage of all true positive cases

$$Recall = \frac{True\ Positive}{True\ Positive + False\ Negative}$$

F1 score

One statistic that balances these features is the harmonic mean of recall and precision.

$$F1score = 2 * \frac{precision * recall}{precision + recall}$$

In neuroblastoma imaging, the GLCM is a powerful tool for extracting texture features from images. These features can provide valuable information about the texture and structure of tissues

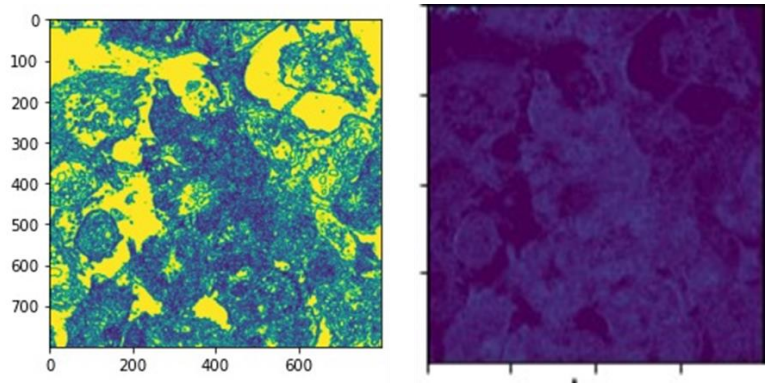

Fig. 5 Energy, dissimilarity

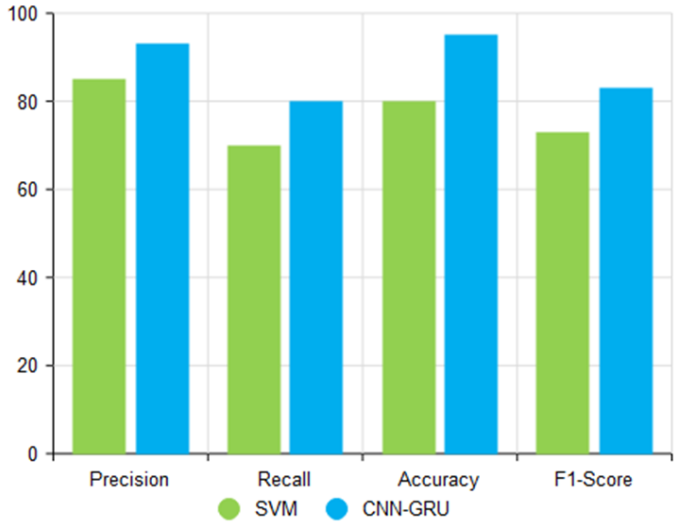

Fig. 6 Performance analysis proposed pediatric cancer

Table 1 Performances metrics

Methods	Precision	Recall	Accuracy	F1- score
SVM	85%	70%	80%	73%
CNN-GRU	93%	80%	95%	83%

or cancer. The GLCM method produced the features of Contrast, entropy, homogeneity, Energy, and dissimilarity which are shown in Figs. 4 and 5.

The Table 1 illustrates SVM classification reached 85% accuracy, 70 % recall and 80 % accuracy and 73 % F1 indicating that it can detect true positively, but it has low recall and thus many true positives are not detected. On the other hand, CNN-GRU is much better in relation to SVM in all metrics with the precision of 93%, recall of 80 %, accuracy of 95 %, and F1-score of 83 %. The greater accuracy is expressed in the number of false positives and the greater the recall is expressed in the number of true cases which reduces the false negatives. It is noteworthy that its

accuracy has increased significantly, which proves its robustness, and that the F1-score demonstrates that the precision and the recall are very strong. These findings suggest that CNN-GRU model is more efficient and valid, provides more generalization, and better predictive abilities to the specified domain of problems.

The performance analysis of neuroblastoma pediatric cancer using a hybrid CNN-GRU algorithm produced precision, recall, accuracy, and F1-score which is shown in Figure 6. SVM results demonstrate moderate accuracy with 85% precision, 70% recall, 80% accuracy and 73% F1-score, which implies the low detection performance. The proposed CNN-GRU, in its turn, demonstrates a higher accuracy, 95% precision, 80% recall, and 93% F1-score, which is better than SVM in every aspect. False positives and false negatives are minimized by the increased accuracy and recall of CNN-GRU.

5. Conclusions

In conclusion, the integration of the Wiener filter, GLCM feature extraction, and CNN-GRU classification provides a robust framework for analyzing neuroblastoma in pediatric cancers. Wiener filter improves image quality by reducing noise, thereby enhancing the reliability of downstream analyses. GLCM feature extraction captures crucial texture details of neuroblastoma cancers, offering insights into their structural characteristics. These texture features, along with those extracted by Convolutional Neural Network (CNN) for spatial patterns, are then processed by a Gated Recurrent Unit (GRU) to handle any temporal or sequential aspects. The combined CNN-GRU model leverages spatial and temporal information to accurately classify and differentiate neuroblastoma cases. The CNN-GRU achieved efficient results as precision, recall, accuracy, and F1-score of 93%, 80%, 95%, and 83%.

References

Al-Hussaini, I., White, B., Varmeziar, A., Mehra, N., Sanchez, M., Lee, J., ... and Mitchell, C.S. (2024), "An interpretable machine learning framework for rare disease: a case study to stratify infection risk in pediatric leukemia". *J. Clinic. Med.*, **13**(6), 1788. https://doi.org/10.3390/jcm13061788.

Artzi, M., Redmard, E., Tzemach, O., Zeltser, J., Gropper, O., Roth, J., ... and Ben-Sira, L. (2021), "Classification of pediatric posterior fossa tumors using convolutional neural network and tabular data". *IEEE Access*, **9**, 91966-91973. https://doi.org/10.1109/ACCESS.2021.3085771.

Attallah, O. (2021), "MB-AI-His: histopathological diagnosis of pediatric medulloblastoma and its subtypes via AI". *Diagnostics*, **11**(2), 359. https://doi.org/10.3390/diagnostics11020359

Bohannan, Z.S., Coffman, F. and Mitrofanova, A. (2022), "Random survival forest model identifies novel biomarkers of event-free survival in high-risk pediatric acute lymphoblastic leukemia", *Comput. Struct. Biotech. J.*, **20**, 583-597. https://doi.org/10.1016/j.csbj.2022.01.003.

Chadaga, K., Prabhu, S., Sampathila, N. and Chadaga, R. (2023), "A machine learning and explainable artificial intelligence approach for predicting the efficacy of hematopoietic stem cell transplant in pediatric patients". *Healthcare Anal.*, **3**, 100170. https://doi.org/10.1016/j.health.2023.100170.

Cheng, Z.J., Li, H., Liu, M., Fu, X., Liu, L., Liang, Z., ... and Sun, B. (2024), "Artificial intelligence reveals the predictions of hematological indexes in children with acute leukemia", *BMC Cancer*, **24**(1), 993. https://doi.org/10.1371/journal.pone.0320669.

Chounta, S., Allodji, R., Vakalopoulou, M., Bentriou, M., Do, D.T., De Vathaire, F., ... and Letort Le Chevalier, V. (2023), "Dosiomics-based prediction of radiation-induced valvulopathy after childhood

cancer", *Cancers*, **15**(12), 3107.https://doi.org/10.3390/cancers15123107.

Hamd, Z.Y., Osman, E.G., Alorainy, A.I., Alqahtani, A.F., Alshammari, N.R., Bajamal, O., ... and Khandaker, M.U. (2024), "The role of machine learning in detecting primary brain tumors in Saudi pediatric patients through MRI images", *J. Radiat. Res. Appl. Sci.*, **17**(3), 100956. https://doi.org/10.1016/j.jrras.2024.100956.

Horan, M.R., Sim, J.A., Krull, K.R., Ness, K.K., Yasui, Y., Robison, L.L., ... and Huang, I. C. (2023), "Ten considerations for integrating patient-reported outcomes into clinical care for childhood cancer survivors", *Cancers*, **15**(4), 1024. https://doi.org/10.3390/cancers15041024.

Jahangiri, L. (2024), "Predicting neuroblastoma patient risk groups, outcomes, and treatment response using machine learning methods: a review", *Med. Sci.*, **12**(1), 5. https://doi.org/10.3390/medsci12010005.

Jian, C., Chen, S., Wang, Z., Zhou, Y., Zhang, Y., Li, Z., ... and Gong, J. (2023), "Predicting delayed methotrexate elimination in pediatric acute lymphoblastic leukemia patients: An innovative web-based machine learning tool developed through a multicenter, retrospective analysis", *BMC Med. Inform. Decision Making*, **23**(1), 148. https://doi.org/10.1186/s12911-023-02248-7.

Jiwani, N., Gupta, K., Pau, G. and Alibakhshikenari, M. (2023), "Pattern recognition of acute lymphoblastic leukemia (ALL) using computational deep learning". *IEEE Access*, **11**, 29541-29553. https://doi.org/10.1109/ACCESS.2023.3260065.

Kifle, N., Teti, S., Ning, B., Donoho, D.A., Katz, I., Keating, R. and Cha, R.J. (2023), "Pediatric brain tissue segmentation using a snapshot hyperspectral imaging (sHSI) camera and machine learning classifier", *Bioengineering*, **10**(10), 1190. https://doi.org/10.3390/bioengineering10101190.

Li, W., Xia, Y., Wang, J., Jin, H. and Li, X. (2024), "Prognostic significance of migrasomes in neuroblastoma through machine learning and multi-omics", *Sci. Rep.*, **14**(1), 16629. https://doi.org/10.3389/fbinf.2022.954529.

Pacchiano, F., Tortora, M., Doneda, C., Izzo, G., Arrigoni, F., Ugga, L., ... and Brunetti, A. (2024), "Radiomics and artificial intelligence applications in pediatric brain tumors", *World J. Pediatr.*, **20**(8), 747-763.https://doi.org/10.1007/s12519-024-00823-0.

Prashantha, S.J. and Prakash, H.N. (2021), "A features fusion approach for neonatal and pediatrics brain tumor image analysis using genetic and deep learning techniques", *Int. J. Online Biomed. Eng.*, **17**(11). https://doi.org/10.3390/cancers15164172.

Ramesh, S., Chokkara, S., Shen, T., Major, A., Volchenboum, S.L., Mayampurath, A. and Applebaum, M.A. (2021), "Applications of artificial intelligence in pediatric oncology: a systematic review", *JCO Clinic. Cancer Inform.*, **5**, 1208-1219. https://doi.org/10.1200/CCI.21.00102.

Steyaert, S., Qiu, Y.L., Zheng, Y., Mukherjee, P., Vogel, H. and Gevaert, O. (2023), "Multimodal deep learning to predict prognosis in adult and pediatric brain tumors", *Commun. Med.*, **3**(1), 44. https://doi.org/10.1038/s43856-023-00276-y.

Talaat, F.M. and Gamel, S.A. (2023), "A2M-LEUK: Attention-augmented algorithm for blood cancer detection in children", *Neural Comput. Appl.*, **35**(24), 18059-18071. https://doi.org/10.1007/s00521-023-08678-8.

Tozzi, A.E., Eckley, M., Croci, I., Dell'Anna, V.A., Colantonio, E. and Mastronuzzi, A. (2022), "Gaps and opportunities of artificial intelligence applications for pediatric oncology in european research: A systematic review of reviews and a bibliometric analysis", *Front. Oncology*, **12**, 905770. https://doi.org/10.3389/fonc.2022.905770.

Vekariya, V., Passi, K. and Jain, C.K. (2022), "Predicting liver cancer on epigenomics data using machine learning", *Front. Bioinform.*, **2**, 954529. https://doi.org/10.3389/fbinf.2022.954529

Voicu, I.P., Dotta, F., Napolitano, A., Caulo, M., Piccirilli, E., D'Orazio, C., ... and Colafati, G.S. (2024), "Machine learning analysis in diffusion kurtosis imaging for discriminating pediatric posterior fossa tumors: A repeatability and accuracy pilot study". *Cancers*, **16**(14), 2578. https://doi.org/10.3390/cancers16142578.

Yang, J., Wang, J., Tian, S., Wang, Q., Zhao, Y., Wang, B., ... and Ma, J. (2021), "An integrated analysis of tumor purity of common central nervous system tumors in children based on machine learning methods". *Front. Genetics*, **12**, 707802. https://doi.org/10.3389/fgene.2021.707802. eCollection 2021.

Yang, T., Liu, D., Zhang, Z., Sa, R. and Guan, F. (2024), "Predicting T-cell lymphoma in children from 18F-FDG PET-CT imaging with multiple machine learning models", *J. Imag. Inform. Med.*, **37**(3), 952-964. https://doi.org/10.1007/s10278-024-01007-y.

Yearley, A.G., Blitz, S.E., Patel, R.V., Chan, A., Baird, L.C., Friedman, G.K., ... and Bernstock, J.D. (2022), "Machine learning in the classification of pediatric posterior fossa tumors: A systematic review", *Cancers*, **14**(22), 5608.https://doi.org/10.3390/cancers14225608.

Yoon, H.J., Peluso, A., Durbin, E.B., Wu, X.C., Stroup, A., Doherty, J., ... and Penberthy, L. (2022), "Automatic information extraction from childhood cancer pathology reports", *JAMIA Open*, **5**(2), ooac049. https://doi.org/10.1093/jamiaopen/ooac049.

Zhang, I.Y., Hart, G.R., Qin, B. and Deng, J. (2023), "Long-term survival and second malignant tumor prediction in pediatric, adolescent, and young adult cancer survivors using Random Survival Forests: a SEER analysis", *Sci. Rep.*, **13**(1), 1911. https://doi.org/10.1038/s41598-023-29167-x.

Zhang, L., Gao, H. J., Zhang, J. and Badami, B. (2020), "Optimization of the convolutional neural networks for automatic detection of skin cancer", *Open Med.*, **15**(1), 27-37. https://doi.org/10.1515/med-2020-0006.

Zheng, Y., Zhang, C., Sun, X., Kang, K., Luo, R., Zhao, A. and Wu, Y. (2024), "Survival trend and outcome prediction for pediatric Hodgkin and non-Hodgkin lymphomas based on machine learning", *Clinic. Experim. Med.*, **24**(1), 132. https://doi.org/10.1007/s10238-024-01402-3.

Zijtregtop, E.A., Winterswijk, L.A., Beishuizen, T.P., Zwaan, C.M., Nievelstein, R.A., Meyer-Wentrup, F.A. and Beishuizen, A. (2023), "Machine learning logistic regression model for early decision making in referral of children with cervical lymphadenopathy suspected of lymphoma". *Cancers*, **15**(4), 1178. https://doi.org/10.3390/cancers15041178.

PR